




Research Article

Laser polished fused deposition poly-lactic acid objects for personalized orthopaedic application

Yuan Chai¹ · Xiao-Bo Chen² · Donghai Zhang¹ · Joseph Lynch¹ · Nick Birbilis³ · Qing-Hua Qin³ · Paul N. Smith⁴ · Rachel W. Li^{1,5} 

Received: 26 June 2020 / Accepted: 7 October 2020 / Published online: 17 October 2020
© The Author(s) 2020 

Abstract

Patient-specific surgical guides are increasingly demanded. Material Extrusion (ME) is a popular 3D printing technique to fabricate personalized surgical guides. However, the ME process usually generates deleterious surface topography which is not suitable for orthopaedic emergencies. We designed and optimized parametric combinations of a laser polishing approach as post process to improve the surface quality of ME-made poly-lactic acid (PLA) objects. In this study, we investigated the contribution of processing variables to the mechanical properties and the biocompatibilities in vitro of the ME-made PLA objects. Conventional surface grinding was conducted as comparison. The results demonstrate that the ME-made PLA samples exhibit good mechanical properties and favourable biocompatibility after being post processed using laser polishing. The post laser polishing, as a powerful tool in manufacture of ME-made PLA objects, will open a new approach with a great promise in its applications in personalized and timely management of medical emergencies.

Keywords Biocompatibility · Fused deposition modelling · Mechanical strength · Orthopaedics · Surgical guide · Three dimensional printing

1 Introduction

Orthopaedic implants and surgical guides are usually standardized products that are categorized into a limited number of sizes to fit all patients [1]. However, bone geometrical and structural parameters and the complexity of a traumatic injury or joint reconstruction vary individually [2, 3]. Consequently, the geometric mismatch between a surgical device and individual bone increases the possibility of nerve roots or visceral damage [4, 5], biomechanical disadvantages [6], implant mobility and loosening [7], and implant failure [8]. Good fitting accuracy of implants or surgical guides will reduce the risk of body rejection and

complications, and influence on the osseointegration at the interface between bone and implants after surgery, which will largely improve clinical outcomes. Therefore, customized patient-specific medical implants with an accurate implant configuration and appropriate implant placement have become attractive [9]. Likewise, patient-specific surgical guides are increasingly demanded, particularly by orthopaedic surgeons worldwide in planning their surgeries and improving the accuracy during their performances [10].

Three-dimensional (3D) printing, a modern additive manufacturing technology, emerges as a simple and feasible solution to the manufacturing issue related to

✉ Rachel W. Li, rachel.li@anu.edu.au | ¹Trauma and Orthopaedic Research Laboratory, Department of Surgery, The Medical School, The Australian National University, Canberra, ACT 2601, Australia. ²School of Engineering, RMIT University, Carlton, VIC 3053, Australia. ³Research School of Engineering, College of Engineering and Computer Science, Australian National University, Canberra, ACT 2601, Australia. ⁴Trauma and Orthopaedic Research Unit, The Canberra Hospital, Yamba Drive, Garran, ACT 2605, Australia. ⁵Department of Immunology and Infectious Disease, John Curtin School of Medical Research, The Australian National University, Acton, ACT 0200, Australia.



medical devices that are highly demanded by medical field, particularly in orthopaedic emergencies because it buildspatient-specific models and fabricate surgical guides and implants. To date, material extrusion (ME) is the most commonly used and the most accessible 3D printing technology for customized medical applications [11]. A hot-end tip extrudes melted material filament which solidifies at the designated spatial position of a proposed 3D model. This technique allows physical fabrication from a computer-aid-design (CAD) model at a relatively low cost [12].

Poly-lactic acid (PLA) is one of the most commonly used thermoplastic materials in ME printing which has been shown to have sufficient geometrical accuracy [13], strength resistance and good biocompatibility in vitro [14, 15]. ME prototypes have been used successfully as guiding instruments to assist surgical procedures [16–18]. However, a number of limitations still exist. Research showed that the ME process changes the chemical properties of the original PLA, making it more susceptible to degradation in physiological conditions [19]. Such PLA objects exhibit a rough surface topography, specifically a staircase surface texture with a low directional resolution [20, 21]. Surface roughness of a bio-material is essential to its mechanical strength and cell growth [22]. Poor surface quality of the ME-made PLA parts that contains the deleterious staircase structure constrains their application as a final product for medical applications. Other than improving the surface quality by optimizing the processing parameters [23, 24], post surface treatment reduces the deleterious staircase surface characteristics of ME products, which can be directly quantified by a reduction of surface roughness. Studies have investigated different post processing methods for improving surface quality of the ME products [25, 26], such as barrel finishing, vapour smoothing and chemical etching techniques [27, 28]. These methods are currently offering available options for post surface processing on the ME-made PLA parts. However, the disadvantages, such as chemical contamination, high production cost and long processing time length make them impractical to the use in emergent medical situations, like trauma management.

Laser scanning for post polishing of metal 3D printing prototypes has been widely used [29, 30]. Although the laser treatment usually applies on polishing of flat surface because of its technical nature, the laser polishing is greatly desired for medical device manufacturing because it possesses contactless and wearless machining abilities and penetrates material surface to polish the inner structure [31–33]. Our laboratory and other researchers developed a novel laser polishing method on polymer 3D printed object, and conducted preliminary studies [34, 35]. Although researchers have reported the mechanical

strength of PLA composite with or without laser polishing, the mechanical and biocompatible behaviours of laser post processed ME-made PLA object have not been fully investigated [36, 37]. Its feasibility on orthopaedic application remains unknown. In this study, we explored the contribution of processing variables to the mechanical properties and biocompatibilities of ME-made PLA and identified the optimal set of laser scanning parameters. Conventional mechanical grinding was conducted as comparison. We expect to provide comprehensive experimental evidence to support the post laser polishing as a powerful tool in manufacture of ME-made PLA objects for the use in personalized and timely management of medical emergencies.

2 Material and methods

2.1 3D printing

As demonstrated in Fig. 1, the 3D model contains three different parts to fill in a solid material. The first part is a brim, i.e. fringe of a model at each layer, where the extruder scans. The second part is infill, in which the inside area of the model is filled by a proposed pattern and density. The third part is a supporting structure which refers to the features that do not exist in the 3D model, but support the upper layer to maintain its spatial position. The 3D model was designed using Solidworks (Dassault Systemes SA, France), and were converted to.stl file to be recognizable by the 3D printer. The slicing strategy was generated using the software Simplify3D (Simplify3D, OH, USA). To examine the mechanical properties of the ME-made PLA objects and post processed with the laser scanning, we designed

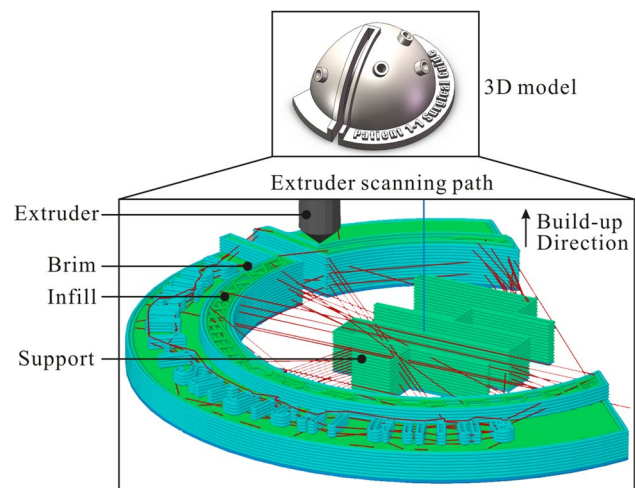


Fig. 1 Schematic diagram of 3D printing

model geometries based on the requirements of International Organization for Standardization (ISO). We prepared samples for tensile and compression tests and flexural properties under the defined conditions according to the standards of ISO 527 [38], ISO 604 [39], and ISO 178 [40], respectively. In addition to the mechanical tests, we also prepared sample discs for in vitro biocompatibility test at 12 mm radius and 1.5 mm thickness, with a surface area of 1.02 cm². These parameters were determined according to ISO 10,993–5 [41], including the requirement of a ratio between the size of test sample and density of cell seeding. This study focuses on the mechanical and biocompatible comparison of post treated samples, thus the influence of complex sample geometry is not discussed.

We used an aluminium frame reinforced self-assembly deltabot ME 3D printer to manufacture PLA components for surface polishing experiments. We selected white PLA filaments with a 1.75 mm (Sunhokey-tec, Guangdong, China) as stock materials owing to their good thermal performance and environmentally friendly nature. During ME process, samples for mechanical testing were oriented flatly and for interlayer bonding were oriented vertically. Parameters were set as 195 °C extrusion temperature and 60 °C bed temperature, 60 mm/s printing speed, 70% infill density and rectilinear infill pattern with double brim. In contrast, samples for biocompatibility testing were printed vertically and made in 100% solid infill to avoid hollow interior. All models were sliced at 0.25 mm layer thickness.

2.2 Post processing using laser scanning

We used a 40 W laser scanning machine (King Rabbit HX-40A, Shandong, P.R. of China) and a mechanical grinding machine to prepare the test samples. To achieve shallow melt regime on the surface, we used a set of the parameters of laser polishing treatment at 3 W output power, 0.025 mm scan line gap, 30 ms delay between pulses, and 150 mm/s scan speed as previously described [35]. A square area that fully covered the sample was scanned by laser and each laser pulse scanned along the short side. Samples were post processed at all sides of faces. A 700 grit sandpaper was applied with water as lubricant at a rotation speed of 150 r/min for mechanical surface grinding. Although the manually controlled grinding pressure could hardly be quantified to a standard procedure, we optimised and set the grinding duration at 40–50 s/corresponding side. A grinding depth of 0.25 mm was achieved at each side.

2.3 Validation of surface roughness

A Wyko NT1100 optical profiler (Veeco, AZ, USA) was used to determine the surface roughness (S_a) (μm) of the

ME-made PLA samples before and after post surface treatment [42], shown below:

$$S_a[\mu m] = \frac{1}{A} \iint_A |z_{(x,y)}| dx dy \quad (1)$$

The effectiveness of the topography optimization was evaluated by the roughness reduction of surface (%), shown below:

$$S_{a_{reduction}} [\%] = \frac{S_{a_{initial}} - S_{a_{polished}}}{S_{a_{initial}}} \times 100 \quad (2)$$

An area of 1.3 × 0.9 mm² that contained over 5 layers of waviness on each sample was scanned to calculate the overall surface roughness. The same area of scan was applied on measuring the grinded samples that had no obvious waviness.

2.4 Mechanical properties

An Instron mechanical tester (Instron®4505, MA, USA) was employed for investigating tensile, compression and flexure properties of the PLA parts at room temperature, 23 °C and 50% relative humidity according to the standards of ISO 527. To quantify mass loss during the laser polishing treatment, the samples were weighted before and after the post processing on an electronic balance with an accuracy of 0.0001 g. In tensile test, velocity was 5 mm/min and the specimen was loaded until it was broken with a load cell of 5 kN. In compression test, cross-sectional dimensions after post processing were measured using a 50 kN load cell and velocity at 1.3 mm/min. We used the same load cell for flexural test at a speed of 2 mm/min. The three point bending method was used, with a load cell of 5 kN and a speed of 2 mm/min, to calculate the flexural modulus.

2.5 Biocompatibility testing

We further investigated cytotoxicity of the various ME-made PLA samples in vitro by culturing bone cells on their surface [41]. Three groups of PLA disks were used in this study, i.e. laser scanning polished, as-printed and mechanical grinded discs (control groups). Sample discs were immersed in deionized water for ultrasonic cleaning for 20 min, and irradiated with UV light for 30 min on each side for further use.

Human primary osteoblast cells (OBs), human osteoclast cells (OCs) and human Saos-2 cell line supplied by ECACC (Sigma, Melbourne, Australia) were used in in vitro cytotoxicity test. The human primary OBs were derived from normal human trabecular bone specimens as we previously

described with mild modifications [8], with the permission of the Australia Capital Territory (ACT) Health Human Research Ethics Committee (Ref. ETH.9.07.865). To assess whether the different material discs influence on OB cell growth, the cells were seeded at a density of 5×10^3 cells per well in 1 mL of cell culture medium in 24-well plate containing discs. The cells were cultured at 37 °C, 5% CO₂ for 3 days before were measured for cell density. The experiments were performed at triplicates in each sample group. At the end point, the cells were washed, trypsinized, and resuspended in cold PBS. The cells were counted using Vi-CELL™ Cell Viability Analyser (Beckman Coulter, IN, USA). Cell numbers represented the quantity of surviving cells on each disc.

The human OCs were induced from “buffy coat” (a 42-year-old male volunteer) provided by Australian Red Cross Blood Service with approval from Human Research Ethics Committee of Australian National University (Ref. 2014/253). Peripheral blood mononuclear cells (PBMCs) were separated from the buffy coat as we described previously [43], and approximately 2.5×10^5 cells were placed in a well of 12-well plate containing the sample disc in 1 mL of OC conditional culture medium. The medium is a α -MEM based with supplements of 10% FCS and antibiotics, 10×10^{-9} M dexamethasone Sigma-Aldrich, Australia), 25 ng mL⁻¹ human M-CSF (Merck Millipore, Australia), and 10×10^{-9} M 1,25(OH)₂D₃ (Sigma-Aldrich, Australia). Cell culture medium was refreshed every 2 days. The OC inductive medium supplemented with recombinant human RANKL (Merck Millipore) at 50 ng mL⁻¹ was used and the induced OCs were measure at the day 8 of culture. In the Vi-CELL™ Cell Viability Analyser, we set 70 μ m filter for cells selected as induced matured/prematured OCs. Three independent experiments were performed by two independent researchers.

2.6 Statistical analysis

Experimental data were analysed using software Graphpad Prism7.0 (GraphPad Software, Inc. CA, USA). Student t-test was performed to analyse differences between two means in the experiments. Data is Gaussian distribution without equal standard deviations (SDs) for unpaired comparison. Welch's correction was applied. The statistical significance was set at $p \leq 0.05$. Three to six replicates of each experiment were performed.

3 Results and discussion

3.1 Surface morphologies of post treatment

Surface roughness of FDM-made PLA samples polished by laser scanning and grinding are shown in Table 1. The laser

scanning reduced 47% surface roughness and the grinding 94%. We noted that the surface roughness reduction was not as much as that on laser polishing metal material, laser treatment of polymer still has great potential when it attract more researchers. The profiles of cross-sectional surfaces are shown in Fig. 2. As-printed PLA surface and laser treated surface present a heterogeneous character. We noted that laser scanning evaporated a thin layer of surface material in Figs. 2a, b. We further measured the height difference of a single layer between as-printed area and laser scanned area in Fig. 2c, the later showed a surface roughness at 9.78 μ m. We found that the laser evaporated area declined 24.18 ± 4.28 μ m compared to that of as-printed ($n = 5$ per group). The result indicates that parameters of laser polishing treatment that we set for this project induced ignorable material evaporation.

In this study, only the flat surfaces were laser treated due technology and equipment limitation. Studies reported successful applying laser surface treatment onto curved or complex surface geometry. We planned further investigation about the influence of different sample geometries on laser polishing outcome [44, 45]. It worth to note that a sample at high area-volume ratio may not be suitable to apply laser processing method to improve the surface quality, such as lattice structure. Although the geometry is rare in surgical guide design, an alternative surface treatment method might be required, such as vapour smoothing [28].

3.2 Influence of laser polishing on tensile stress

Slight weight reduction is a common phenomenon after post surface processing. In this study, we measured the weight of samples from all groups and found that both laser and grinding treatments reduced the weight of samples as showed in Table 2. Next, we compared the tensile properties of laser treated samples to that of as-printed and grinded samples as showed in Table 2. There was no significant difference in tensile strain and Young's modulus at break in the samples post processed either using laser polishing or grinding when compared with the as-printed samples. Even though the weight of samples was reduced

Table 1 Surface roughness of samples with different post treatments

Surface type	Surface roughness (μ m)	Roughness reduction (%)
As-printed	14.42 ± 2.55	
Laser treated	7.68 ± 0.65	47
Grinded	0.88 ± 0.18	94

Data represent mean of 3 replicates, \pm SD

by laser treatment from 7.52 to 6.98 g (7.18%), the ultimate tensile stress (UTS) was not significantly influenced ($p > 0.05$).

Technical schematic diagrams are presented in Fig. 3a, which demonstrates samples geometry, post treated faces, and force direction. The stress–strain curves of the as-printed, laser treated, and grinded samples are shown in Fig. 3b and experimental setup is presented in Fig. 3c.

The morphologies of interlayer breaks are shown in Fig. 3d. The laser treated samples had slightly higher UTS than that of the grinded samples at break as presented by red and blue curves, respectively, in Fig. 3b. Our results suggested that the tensile performance is, to some extent, related to the thickness of outer shell of sample. This is agreed with the results by Bagsik et al. who found that the tensile stress of samples build up in the side direction were higher

Fig. 2 Surface profile. **a** surface roughness, images taken from inverted microscope; **b** Quantitative measurement of surface waviness of 3D printed samples under different post treatment; **c** Surface profile of the peak of a layer

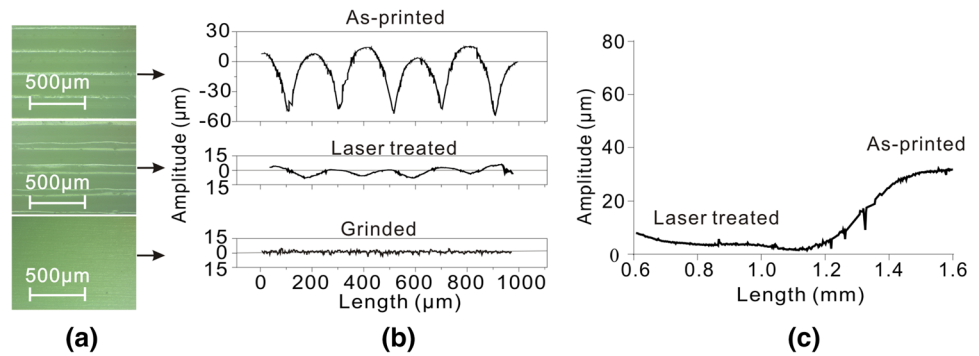


Table 2 Summary of weight and tensile test

	Weight (g)	p	UTS (MPa)	p	Strain at UTS (%)	p	Young's modulus (GPa)	p	Transverse young's modulus(GPa)	p
As-printed	7.52 ± 0.04		28.47 ± 1.30		2.53 ± 0.46		1.15 ± 0.23		0.76 ± 0.12	
Laser treated	6.98 ± 0.01	< 0.01	26.36 ± 2.24	0.25	2.25 ± 0.24	0.41	1.18 ± 0.11	0.87	0.75 ± 0.12	1.00
Grinded	6.23 ± 0.12	< 0.01	21.94 ± 2.10	0.02	2.21 ± 0.16	0.35	0.99 ± 0.04	0.35	0.99 ± 0.06	0.06

UTS, ultimate tensile strength; Data represents mean ± SD of triplicates; p test groups compared to as-printed group

Fig. 3 Tensile test. **a** Schematic of tensile test; **b** Stress–strain curves of FDM specimens with different post processing. Grinded samples had lower ultimate tensile stress at all the three repeats; **c** The experimental setup of tensile; **d** SEM images of the morphologies of the edges at the break interlayer

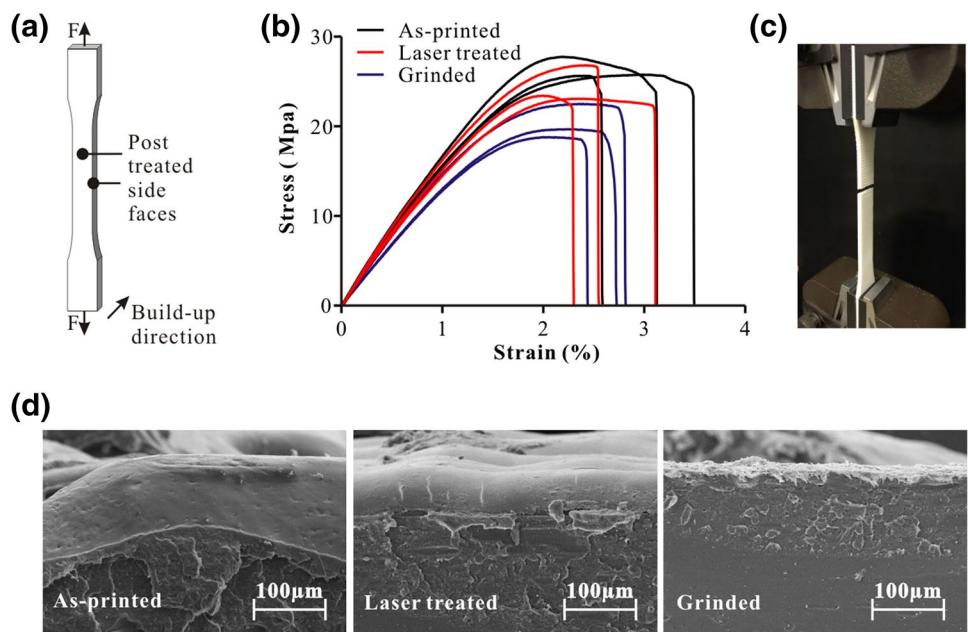
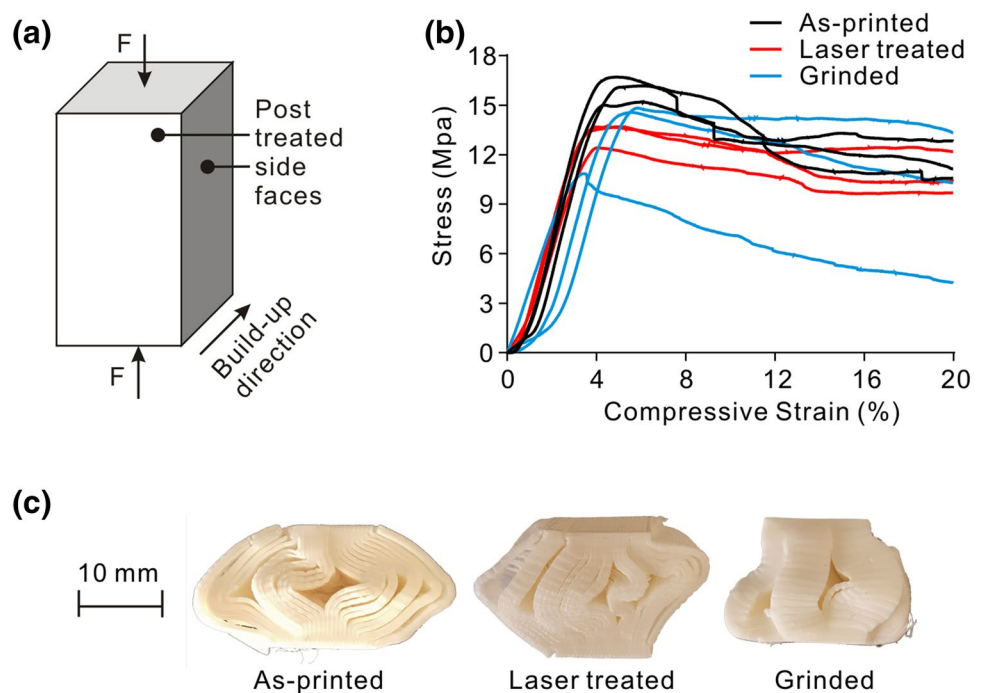


Fig. 4 Compression test. **a** Schematic of compression test; **b** stress–strain curves of FDM specimens with different post processing; **c** Different compressive break morphology of specimens before and after post treatment. More cracks were generated on rougher surface at layer bonding area. Cracks were evenly distributed between layers



than the one build up in the flat direction [46]. The higher tensile stress may also be a result of more build-in shell material along the force direction. This is also ascribed to the low adhesion strength between layers. Further interlayer bonding experiments validated that a more uniform surface makes the object less likely to break at the binding interface between layers, i.e. isotropic surface at low surface roughness. In Fig. 3d, the as-printed sample showed clear border where layers bonded and then broke along. The laser treated sample had flatter waviness, and the border was less clear, but the stress concentration was not reduced. As shown in Table 2, there was no difference between as-printed and laser treated samples ($p = 1.00$), and between as-printed and grinded samples ($p = 0.06$). The raster infill structure can be improved in the software algorithm to change the mechanical property to be suitable for a specific load bearing task [47]. It is worth to note that comparing to the strength of polypropylene which is also widely applied in medical device fabrication, laser treated ME-made PLA samples showed 19.82% higher UTS than that of pure polypropylene samples [48]. This provides supporting evidence to the potential of the proposed surgical guide application.

3.3 Laser polishing achieved favourable compressive stress

To understand the mechanisms that laser treatment achieved a favourable compressive stress, we further

investigated the factors, which could be related to compressive stress, such as weight, deformation morphologies of samples' surface, and infill density. Both post treatments generally reduced the ultimate compressive stress (σ_B) compared with that of as-printed samples as shown in Fig. 4b. As we can see from Table 3, the samples in as-printed group presented the maximum stress. The reduction of maximum σ_B might due to the weight loss during the post processing. The dimensional reduction by surface treatment reduced cross-sectional area. However, it was not sufficient to compensate the decline of compressive stress. This might be an explanation of the σ_B reduction. In addition, there was no statistically significance difference between groups on compressive strain when the samples were broken ($p > 0.05$), regardless of whether the samples were with or without post processing.

Interestingly, we also noted that the deformation morphologies of the samples are different as shown in Fig. 4c. In addition to the Young's Modulus of interlayers that the anisotropic surface is lower than the isotropic surface, this is a further evidence of weak adhesion between the layers when there was no solid infill density. Compressive behaviour in this study is also different from that of a solid material test reported by other researchers [46], in which a break caused by shear strain can be found. This is because our study reduced infill density from 100% solid to 70% to fabricate the samples, which consumed a shorter manufacturing time.

Table 3 Summary of weight and compression test

	Weight (g)	p	Ultimate compressive stress (MPa)	p	Compressive strain at break (%)	p
As-printed	3.21 ± 0.03		16.02 ± 0.73		5.72 ± 0.74	
Laser treated	2.99 ± 0.01	< 0.01	13.26 ± 0.73	0.01	4.35 ± 0.59	0.38
Grinded	2.96 ± 0.08	0.02	13.41 ± 2.22	0.17	4.95 ± 1.28	0.81

Data represents mean ± SD of triplicates; p test groups compared to as-printed group

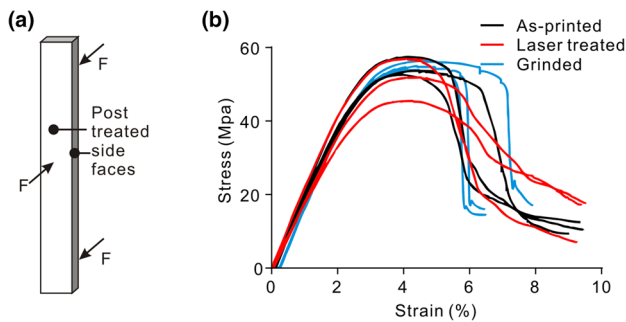


Fig. 5 Flexure test. **a** Schematic of flexure test; **b** Stress–strain curves of ME specimens with different post processing. There is no statistically significant difference, but grinded samples exhibited brittle fracture

3.4 Influence of post treatment on flexure stress

We further analysed differences in flexural modulus, flexural stress and flexure strain of ME-made PLA samples post treated using laser and grinding. The laser treated samples demonstrated similar results to the as-printed samples in the flexure test, while the grinded samples exhibited brittle fracture in Fig. 5b. As presented in Table 4, laser treated samples showed no difference in all parameters compared with those of as-printed samples at break ($p > 0.05$). The grinded samples reached brittle fracture as we reported in the last section, but the weight reduction in the samples grinded was in an acceptable range (5%).

However, there is no significant increase on flexure strain at break when samples were post grinded, which was calculated from the deflection correspondent to the maximum load. As shown in Fig. 5b, we noted that the

stress–strain curves of grinded samples (blue curves) declined dramatically at a short deflection. We infer that the heterogeneity surface, surface at high roughness in this study, reduces the overall rigidity of PLA samples. Therefore, we can conclude that the smoother surface influenced on the flexural capacity of object.

3.5 Laser polishing had less reduction of mechanical properties

There is no statistical difference in Young’s Modulus, flexural modulus, and flexure stress at break. Grinding reduced tensile stress and compressive stress with deformed samples, and laser treatment reduced compressive stress at break. We calculated the reduction of mechanical properties from Table 2, 3, 4. Among all mechanical tests of laser treated samples, a maximum of 17.24% stress reduction at break was found (compression from 16.02 to 13.26 MPa), with an average reduction of 9.40%. Ultimate compression stress was sensitive to the post laser treatment that has statistical reduction ($p < 0.05$). Tensile strength and flexure property on average only reduced 7.41% from 28.47 to 26.36 MPa and 3.56% from 56.89 to 54.87 MPa after laser processing, respectively. In comparison, grinding reduced 16.30% ultimate compressive stress from 16.02 to 13.41 MPa ($p > 0.05$), 22.95% UTS (from 28.47 to 21.94 MPa), and 6.00% flexural stress at break from 56.89 to 53.48 MPa, which on average 5.68% lower than that of laser polished samples.

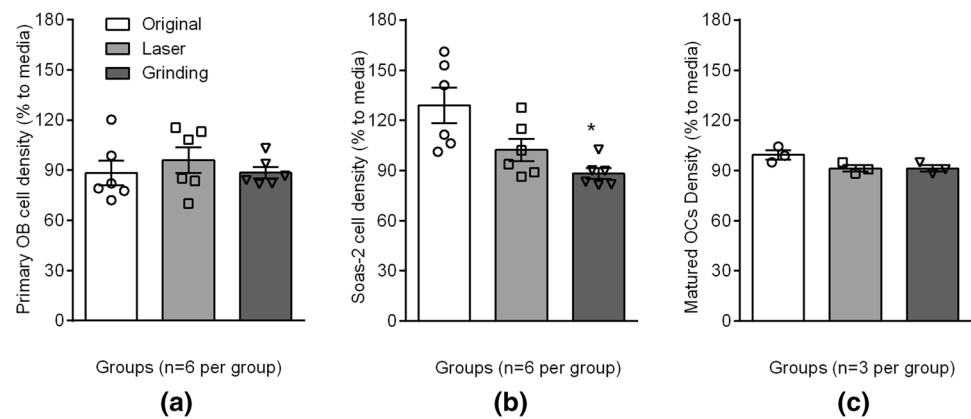
We infer that the post surface treatment made the object more likely to break under compression, and varying material weights might significantly influence the tensile property. However, the resistance to deformation was statistically no difference as shown in all strain analyses.

Table 4 Summary of weight and flexure test

	Weight (g)	p	Flexure stress at break (MPa)	p	Flexure strain at break (%)	p	Flexural modulus (GPa)	p
As-printed	2.70 ± 0.05		56.89 ± 3.76		3.99 ± 0.29		1.32 ± 0.08	
Laser treated	2.70 ± 0.02	0.88	54.87 ± 5.54	0.63	4.04 ± 0.06	0.76	1.21 ± 0.17	0.37
Grinded	2.56 ± 0.03	0.02	53.48 ± 1.50	0.25	4.41 ± 0.11	0.12	1.25 ± 0.01	0.24

Data represents mean ± SD of triplicates; p test groups compared to as-printed group

Fig. 6 In vitro biological test. **a** Cell proliferation of human primary osteoblasts (OBs); **b** Cell proliferation of Saos-2 cells; **c** Matured osteoclasts (OCs). * $p < 0.05$



It was reported and experimentally validated that the E-modulus value of ME-made PLA falls within the range of trabecular bone (0.76–10 GPa) and within the lower limit of cortical bone (3.3–20GPa) [49]. The stiffness of PLA was also suitable for maxillofacial applications [14]. For a surgical guidance that requires geometrical accuracy, we recommend to use laser scanning as a post treatment for a better surface quality. However, if tensile functionality is primarily desired, it is more suitable to use an as-printed object without surface treatment, as long as a smooth surface is not highly required. A more accurate conclusion might be gained by expanding the sample size in further study.

3.6 Laser polishing demonstrated preferable biocompatibility

We next investigated the influence of laser polishing on the biocompatibility of ME-made PLA samples. After being cultured for 3 days, the cell densities of primary OB cells were analysed and compared among groups. As presented in Fig. 6a, although a slightly higher cell density was observed in laser scanning group than that of as-printed and grinding groups, there was no statistical significance when the laser scanning group was compared to the as-printed and the grinding groups ($p = 0.489$ and $p = 0.401$, respectively). From Fig. 6b, we observed that the laser scanning group has no statistically significant influence on Saos-2 cell proliferation compared to the as-printed ($p = 0.058$) and grinding ($p = 0.084$) groups. In contrast, analysis based on the cell density revealed a significant decrease in Saos-2 cells on the surface of grinded samples compared to that of as-printed samples ($p < 0.05$), which might be owing to the surface roughness of grinded samples. These results demonstrate that the samples treated by our designed laser processing parameters are favourable to the growth of bone forming cells. Figure 6c presents the influence of samples tested on the maturation

of human OC cells. The laser scanning group showed no inhibition in the maturation of primary OCs compared to as-printed and grinding groups ($p = 0.074$ and 0.992 , respectively). Those results provide evidences supporting our hypothesis that surface roughness of laser post treated PLA has no toxic effect on either OB or OC cells. The material surface which possesses such a biocompatibility is ideal for use as an intra-operative guidance material in trauma and orthopaedic surgeries.

4 Conclusion

We developed a laser surface scanning for the post processing on ME-made PLA samples and demonstrated that the processed PLA samples exhibited good mechanical properties and favourable biocompatibility. Although no conclusive report, by our knowledge to date, has suggested laser method would be applied to the post surface polishing on the ME-made PLA objects, laser post processing can be a useful option to decrease the processing time in fabricating surgical guides for orthopaedic surgery.

We are planning to conduct further study on validating more properties of laser treated ME samples using different characterizing strategies, and comparing the outcome to other post treatment methods.

Acknowledgements Authors are thankful to Mr. Khu Vu in the Research School Physics, and Dr. Zbigniew Stachurski, Chao Hu and Bobin Xing in the Research School of Engineering at the Australian National University for the technical assistance. This work was Australian Orthopaedic Association Research Foundation AOARF2017.

Compliance with ethical standards

Conflict of interest The authors declare that they have no conflict of interest.

Open Access This article is licensed under a Creative Commons Attribution 4.0 International License, which permits use, sharing,

adaptation, distribution and reproduction in any medium or format, as long as you give appropriate credit to the original author(s) and the source, provide a link to the Creative Commons licence, and indicate if changes were made. The images or other third party material in this article are included in the article's Creative Commons licence, unless indicated otherwise in a credit line to the material. If material is not included in the article's Creative Commons licence and your intended use is not permitted by statutory regulation or exceeds the permitted use, you will need to obtain permission directly from the copyright holder. To view a copy of this licence, visit <http://creativecommons.org/licenses/by/4.0/>.

References

- Gibson I, Rosen DW, Stucker B (2010) Additive manufacturing technologies. Springer, New York
- Petit MA, Beck TJ, Lin HM, Bentley C, Legro RS, Lloyd T (2004) Femoral bone structural geometry adapts to mechanical loading and is influenced by sex steroids: the Penn State Young Women's Health Study. *Bone* 35(3):750–759
- Zengin A, Pye SR, Cook MJ, Adams JE, Wu FC, O'Neill TW, Ward KA (2016) Ethnic differences in bone geometry between white, black and south asian men in the UK. *Bone* 91:180–185
- Carbone JJ, Tortolani J, Quartararo LG (2003) Fluoroscopically assisted pedicle screw fixation for thoracic and thoracolumbar injuries-technique and short-term complications. *Spine* 28(1):91–97
- Austin MS, Vaccaro AR, Brislin B, Nachwalter R, Hilibrand AS, Albert TJ (2002) Image-guided spine surgery-A cadaver study comparing conventional open laminoforaminotomy and two image-guided techniques for pedicle screw placement in posterolateral fusion and nonfusion models. *Spine* 27(22):2503–2508
- Farshad M, Betz M, Farshad-Amacker NA, Moser M (2017) Accuracy of patient-specific template-guided vs free-hand fluoroscopically controlled pedicle screw placement in the thoracic and lumbar spine: a randomized cadaveric study. *Eur Spine J* 26(3):738–749
- Conlisk N, Howie CR, Pankaj P (2017) Computational modeling of motion at the bone-implant interface after total knee arthroplasty: the role of implant design and surgical fit. *Knee* 24(5):994–1005
- Pal N, Quah B, Smith PN, Gladkis LL, Timmers H, Li RW (2011) Nano-osteoimmunology as an important consideration in the design of future implants. *Acta Biomater* 7(7):2926–2934
- Radermacher K, Portheine F, Anton M, Zimolong A, Kaspers G, Rau G, Staudte HW (1998) Computer assisted orthopaedic surgery with image based individual templates. *Clin Orthop Relat Res* 354:28–38
- Di Giacomo GA, Cury PR, de Araujo NS, Sendyk WR, Sendyk CL (2005) Clinical application of stereolithographic surgical guides for implant placement: preliminary results. *J Periodontol* 76(4):503–507
- Wohlers T (2016) Wohlers Report 2016—3D printing and additive manufacturing state of the industry—annual worldwide progress report. 2016. Wohlers Associates, Inc
- Rankin TM, Giovinco NA, Cucher DJ, Watts G, Hurwitz B, Armstrong DG (2014) Three-dimensional printing surgical instruments: are we there yet. *J surg res* 189(2):193–197
- Petropolis C, Kozan D, Sigurdson L (2015) Accuracy of medical models made by consumer-grade fused deposition modelling printers. *Plast Surg* 23(2):91–94
- Wurm MC, Möst T, Bergauer B, Rietzel D, Neukam FW, Cifuentes SC, von Wilmsky C (2017) In-vitro evaluation of Polylactic acid (PLA) manufactured by fused deposition modeling. *J biol eng* 11(1):29
- Juneja M, Thakur N, Kumar D, Gupta A, Bajwa B, Jindal P (2018) Accuracy in dental surgical guide fabrication using different 3-D printing techniques. *Addit Manuf* 22:243–255
- Wang Y-T, Yu J-H, Lo L-J, Hsu P-H, Lin C-L (2017) Developing customized dental miniscrew surgical template from thermoplastic polymer material using image superimposition, cad system, and 3d printing. *BioMed Res Int*. <https://doi.org/10.1155/2017/1906197>
- Ebrahimzadeh A, Azimifar F, Nosouhi R (2016) Design and manufacturing of integrated drilling and cutting orthopedic bone-specific surgical guide. *Mater Manuf Process* 31(5):608–611
- Kunz M, Waldman SD, Rudan JF, Bardana DD, Stewart AJ (2012) Computer-assisted mosaic arthroplasty using patient-specific instrument guides. *Knee Surg Sport Traumatol Arthrosc* 20(5):857–861
- Cuiffo MA, Snyder J, Elliott AM, Romero N, Kannan S, Halada GP (2017) Impact of the fused deposition (fdm) printing process on polylactic acid (pla) chemistry and structure. *Appl Sci* 7(6):579
- Pandey PM, Reddy NV, Dhande SG (2003) Improvement of surface finish by staircase machining in fused deposition modeling. *J Mater Process Technol* 132(1):323–331
- Durgun I, Ertan R (2014) Experimental investigation of FDM process for improvement of mechanical properties and production cost. *Rapid Prototyp J* 20(3):228–235
- Deligianni DD, Katsala N, Ladas S, Sotiropoulou D, Amedee J, Misirlis YF (2002) Effect of surface roughness of the titanium alloy Ti-6Al-4V on human bone marrow cell response and on protein adsorption. *Biomaterials* 22(11):1241–1251
- Sreedhar P, Mathikumar Manikandan C, Jothi G (2012) Experimental investigation of surface roughness for fused deposition modeled part with different angular orientation. *Int J Adv Des Manuf Technol* 5:21–27
- Altan M, Eryildiz M, Gumus B, Kahraman Y (2018) Effects of process parameters on the quality of PLA products fabricated by fused deposition modeling (FDM): surface roughness and tensile strength. *Mat Test* 60(5):471–477
- Galantucci LM, Lavecchia F, Percoco G (2009) Experimental study aiming to enhance the surface finish of fused deposition modeled parts. *CIRP Ann Manuf Technol* 58(1):189–192
- Gajdos I, Slota J (2010) Improving surface finish quality of FDM prototypes. *Zeszyty Naukowe Politechniki Rzeszowskiej Mechanika* 80(274):87–90
- Boschetto BA, Bottini L (2015) Surface improvement of fused deposition modeling parts by barrel finishing. *Rapid Prototyp J* 21(6):686–696
- Chohan JS, Singh R (2016) Enhancing dimensional accuracy of FDM based biomedical implant replicas by statistically controlled vapor smoothing process. *Prog Addit Manuf* 1(1–2):105–113
- Wang D, Wen CY, Chang YN, Lin W, Chen SC (2018) Ultrafast laser-enabled 3D metal printing: a solution to fabricate arbitrary sub-micron metal structures. *Precis Eng-J Int Soc Precis Eng Nanotechnol* 52:106–111
- Kurella A, Dahotre NB (2005a) Review paper: surface modification for bioimplants: the role of laser surface engineering. *J Biomater Appl* 20(1):5–50
- Rosa B, Mognol P, Hascoët J-y (2015) Laser polishing of additive laser manufacturing surfaces. *J Las Appl* 27(S2):S29102
- Gharbi M, Peyre P, Gorny C, Carin M, Morville S, Le Masson P, Carron D, Fabbro R (2013) Influence of various process conditions on surface finishes induced by the direct metal deposition laser technique on a Ti-6Al-4V alloy. *J Mater Process Technol* 213(5):791–800

33. Kurella A, Dahotre NB (2005b) Surface modification for bioimplants: the role of laser surface engineering. *J Biomater Appl* 20(1):5–50
34. Perez Dewey M, Ulutan D (2017) Development of Laser Polishing As an Auxiliary Post-Process to Improve Surface Quality in Fused Deposition Modeling Parts. Proceedings of the ASME 2017 12th International Manufacturing Science and Engineering Conference collocated with the JSME/ASME 2017 6th International Conference on Materials and Processing. Volume 2: Additive Manufacturing; Materials. Los Angeles, California, USA. June 4–8, 2017. Paper No: MSEC2017-3024, V002T01A006; 6 pages, ASME
35. Chai Y, Li RW, Perriman DM, Chen S, Qin QH, Smith PN (2018) Laser polishing of thermoplastics fabricated using fused deposition modelling. *Int J Adv Manuf Technol* 96(9–12):4295–4302
36. Papon EA, Haque A (2018) Tensile properties, void contents, dispersion and fracture behaviour of 3D printed carbon nanofiber reinforced composites. *J Reinf Plast Compos* 37(6):381–395
37. Chen L, Zhang X (2019) Modification the surface quality and mechanical properties by laser polishing of Al/PLA part manufactured by fused deposition modeling. *Appl Surf Sci* 492:765–775
38. E ISO 527–1 (1996) Plastics—Determination of tensile properties—Part 1: General principles International Organization for Standardization, Geneva, 1996
39. E ISO 604 (2003) Plastics—determination of compressive properties (ISO 604: 2002)
40. Iso S (1997) 178. Plastics, Determination of the bending (in Polish)
41. Wallin RF, Arscott E (1998) A practical guide to ISO 10993–5: Cytotoxicity. *Med Device Diagn Ind* 20:96–98
42. ISO I S O. 25178-2: 2012—Geometrical Product Specifications (GPS)—Surface Texture: Areal—Part 2: Terms, Definitions and Surface Texture Parameters[J]. International Standards Organization: Geneva, Switzerland, 2012
43. Ding YF, Li RW, Nakai M, Majumdar T, Zhang DH, Niinomi M, Birbilis N, Smith PN, Chen XB (2016) Osteoanabolic implant materials for orthopedic treatment. *Adv Healthc Mater* 5(14):1740–1752
44. Anemone G, Weingarten C, Al Taleb A, Prieto C, Fariás D (2017) Ultrasmooth metal thin films on curved fused silica by laser polishing. *Appl Phys Lett* 111(18):181602
45. Yung K, Xiao T, Choy H, Wang W, Cai Z (2018) Laser polishing of additive manufactured CoCr alloy components with complex surface geometry. *J Mater Process Technol* 262:53–64
46. Bagsik A, Schöppner V, Klemp E (2010) FDM part quality manufacture with Ultem* 9085. In: 14th international scientific conference on polymeric materials
47. Sood AK, Ohdar RK, Mahapatra SS (2010) Parametric appraisal of mechanical property of fused deposition modelling processed parts. *Mater Des* 31(1):287–295
48. Sodeifian G, Ghaseminejad S, Yousefi AA (2019) Preparation of polypropylene/short glass fiber composite as fused deposition modeling (FDM) filament. *Results Phys* 12:205–222
49. Mow VC, Huiskes R (2005) Basic orthopaedic biomechanics & mechano-biology, 3rd edn. Lippincott Williams & Wilkins, Philadelphia, PA

Publisher's Note Springer Nature remains neutral with regard to jurisdictional claims in published maps and institutional affiliations.